

Nanoscale structures on ultra-precision machined fluorite surfaces

S Gritschneider¹, Y Namba² and M Reichling¹

¹ Fachbereich Physik, Universität Osnabrück, BarbarasträÙe 7, 49076 Osnabrück, Germany

² Department of Engineering, Chubu University, 1200 Matsumotocho, Kasugai, Aichi 487-8501, Japan

E-mail: reichling@uos.de

Received 10 February 2005, in final form 17 March 2005

Published 19 April 2005

Online at stacks.iop.org/Nano/16/883

Abstract

Highest purity calcium difluoride crystals having a roughness below 1 nm over large areas were prepared by ultra-precision machining to create technical surfaces for optical applications. High resolution dynamic scanning force microscopy reveals surfaces with close to atomic flatness over areas larger than 10 μm^2 . The residual roughness is due to a high density of pits and protrusions with a height of 0.32 nm corresponding to an F–Ca–F triple-layer that is the smallest possible unit on stoichiometric $\text{CaF}_2(111)$. Additionally, imperfections of the machining process may appear as protrusions of typically 1 nm height or a high density of aligned triple-layer steps for surfaces that were apparently slightly inclined with respect to the machining plane. A terraced structure also appears in the vicinity of nanometre-sized defects found for one sample. Machining may also cause a fracture in the form of branched channels of some tens of nanometres in width and some micrometers in length.

(Some figures in this article are in colour only in the electronic version)

1. Introduction

Following the roadmap of the semiconductor industry, a structure size below 50 nm will be standard in microelectronics in 2006, and creating such small structures requires production processes based on 157 nm laser lithography [1–3]. This technology is already available but it has, however, not yet reached a state of maturity needed to be established as an industrial standard. A major obstacle for the further development of photolithography based on deep ultraviolet (DUV) laser light is the problems related to the optical materials used in DUV projection systems [4–6]. In this spectral region, conventional optical materials fail as they are not transparent for the DUV light. Due to its very wide band gap and other convenient material properties, CaF_2 is the material of choice for DUV applications. However, this brittle, single-crystalline material is a severe challenge for lens makers and, therefore, novel manufacturing and testing procedures have to be applied for surface shaping, finishing and analysis [7]. In this contribution we show that, by using ultra-precision grinding and float polishing techniques, it is possible to create well defined surfaces with

minimal surface roughness. We examined the polishing results of six simultaneously processed high purity CaF_2 samples from different sources. Surfaces were investigated by high resolution dynamic scanning force microscopy that had been shown in previous studies to be capable of structural analysis on fluorite with a resolution reaching down to the atomic level [8]. In the present studies, triple layers can be resolved in topographical imaging; however, the lateral resolution is limited to detecting nanometre-sized surface pits and protrusions.

2. Experimental details

We investigated six highest quality CaF_2 samples (labelled a, b, c, d, e, f) of $10 \times 10 \times 7 \text{ mm}^3$ dimensions provided by different vendors. After cleavage along the (111) plane, samples were glued in a circular arrangement onto a stainless steel machining wheel, as shown in figure 1, because we aimed for giving all of them exactly the same machining treatment. The samples were ground using an ultra-precision surface grinder [9] with an SD1500-75-B diamond wheel to obtain a flat plane among

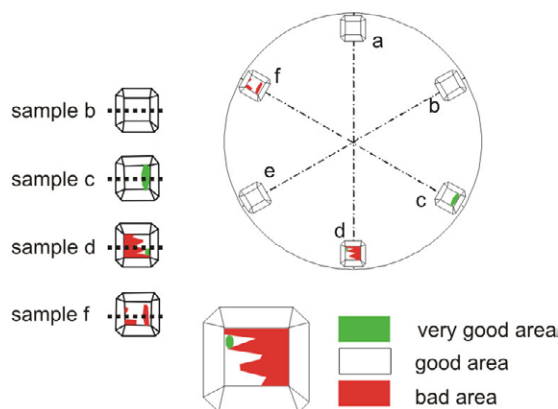


Figure 1. Six samples are symmetrically glued on the machining wheel to give all samples the same machining treatment. SFM measurements were performed at various positions along the dotted lines. The classification of ‘bad’, ‘good’ and ‘very good’ areas is a result of visual inspection with a Nomarski microscope.

the samples. The samples were then polished on a tin lap with $3\ \mu\text{m}$ diamond powder, washed out with pure water and float polished [10] on a tin lap with $7\ \text{nm}$ diameter SiO_2 powder. To avoid contamination during the entire processing chain of polishing, machining, optical inspection, packing, unpacking and introduction into the high vacuum for scanning force microscopy inspection. However, machining results might be influenced by minute variations in sample thickness or misalignment in gluing that are beyond our control. Therefore, the results presented here demonstrate the state of the art and some peculiarities of finishing fluorite surfaces; however, success or failure on individual samples cannot be related to crystal quality. The results from four out of six samples selected for presentation exhibit typical features and can be regarded as representative for the entire set.

Surface topography was determined with a commercial high resolution dynamic scanning force microscope operated in high vacuum in the so-called non-contact mode (NC-SFM) that had been used in previous studies on fluorite [11]. Imaging experiments were performed with FMR-type silicon cantilevers from Nanosensors that have a resonance frequency of $75\ \text{kHz}$. The scanning range of our instrument is limited to an area of $4 \times 4\ \mu\text{m}^2$. As it is not possible to cover the entire sample surface with high resolution, we have taken 2–4 random samples from selected surface areas. To facilitate a rational selection of regions to be investigated, each sample was first inspected by Nomarski microscopy. Based on the judgement of an experienced microscopist, the surface of all samples was subdivided into areas classified as ‘bad’, ‘good’ or ‘very good’, resulting in quality maps as shown in figure 1. Nomarski microscopy reveals micrometre-scale roughness and machining faults but does not yield quantitative results. Hence, the classification provides a guideline for the search of best quality surface areas rather than providing an exact measure for surface quality.

3. Results and discussion

Figure 2, representing results from sample b, shows a typical surface structure as we observe it regularly for good quality

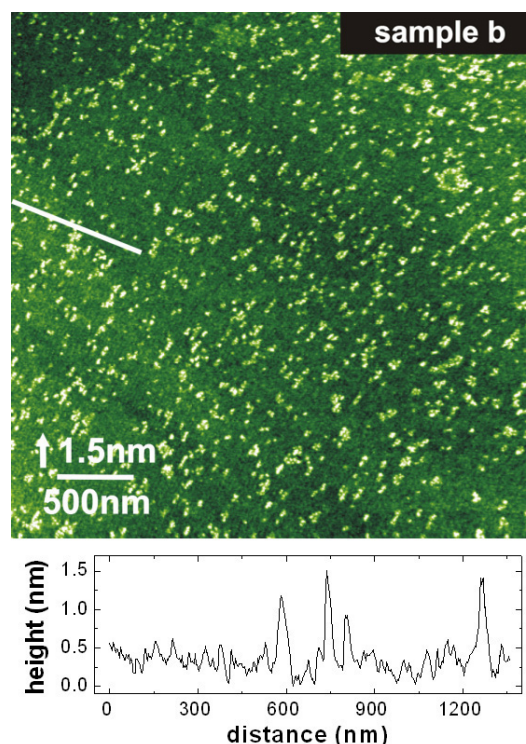


Figure 2. Typical appearance of $10\ \mu\text{m}^2$ of a machined surface as measured on sample b. The nearly atomically flat surface is covered with protrusions (bright spots) that are possibly a leftover from the machining process. Smaller surface features are aligned along unidirectional trenches of yet unidentified origin. Trenches are some nanometres wide and run probably over the entire surface. The line profile reveals the different scales of features determining surface roughness, namely a large number of triple-layer height pits and protrusions with a height of about $300\ \text{pm}$ and a small number of protrusions with a height of $1\text{--}2\ \text{nm}$.

areas. The topographic variation over the entire scanned area of $3.5 \times 3.5\ \mu\text{m}^2$ is extremely small compared to surfaces produced by cleavage or conventional polishing. As the dominant morphological feature, we observe protrusions of up to $1\ \text{nm}$ in height and some nanometres in lateral dimensions that randomly cover the surface.

The resulting RMS roughness of $0.3\ \text{nm}$ as evaluated from image analysis is, however, mainly determined by smaller scale surface features apparent upon closer inspection. Additional to the nanometre protrusions, the image reveals pits and protrusions with a height of about $300\ \text{pm}$ that are not randomly distributed across the surface but often line up along small trenches of a few nanometres width running straight across the surface. The direction of the trenches is the same over the entire machined area; however, we could not clearly identify a specific preparation step as the origin of the trenches. We anticipate that the larger protrusions are formed by leftovers from the surface treatment. A more quantitative analysis of topographic features is facilitated by the height profile included in figure 2. The dominance of up and down steps with $300\ \text{pm}$ height suggest that pits and protrusions are formed of F–Ca–F triple-layers (nominal height $315\ \text{pm}$) that are known to be stable building blocks of the fluorine terminated (111) surface. Best machining results shown in figure 3 were obtained on sample f, where the surface was not

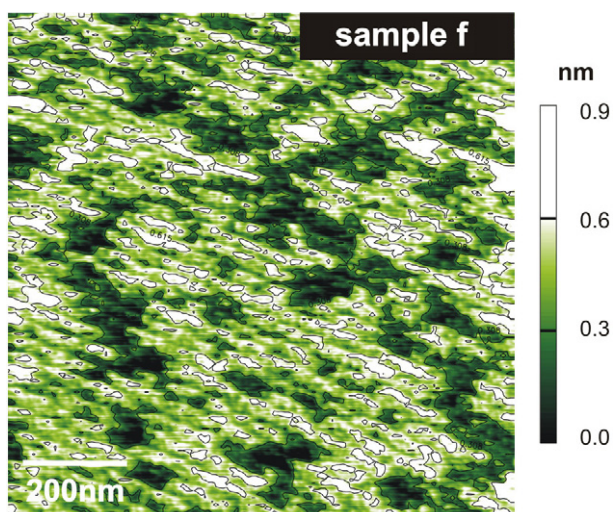


Figure 3. Highly resolved image of $1 \mu\text{m}^2$ in a good area imaged on sample f that yielded the best machining results. The scale bar covering a range of 0.9 nm reveals that all surface features can be associated with three different height levels separated by steps of 0.3 nm height.

found to be contaminated by larger features. This and similar images clearly demonstrate that large areas with a roughness of ± 1 triple-layer can be prepared by precision machining and subsequent float polishing. From the analysis of many scans of up to $10 \mu\text{m}^2$ in size taken at different regions of the crystal surfaces, we conclude that the actual area of nearly atomic flatness can be several hundred μm^2 and more.

A significantly different surface structure shown in figure 4 was found on sample d, exhibiting a regular array of terraces typical for a vicinal surface. The ridge structure found on the other surfaces could not be identified on this sample. The cross-section shown in figure 4 taken perpendicular to the direction of the step edges reveals a height difference of 0.31 nm between terraces, again corresponding to the triple-layer height. For this sample, apparently the machining plane and the (111) plane of the crystal were not well aligned. From the terrace width, we determine an inclination angle of about 5° with respect to the (111) plane that is most probably the result of a mistake when gluing the sample onto the machining wheel.

Other machining-related defect structures found in bad regions of samples d and f that resulted in a tremendously increased surface roughness are shown in figure 5. On sample d, we recognize large defects surrounded by curved terraces having the appearance of height lines. Furthermore, we detect the remainder of a large triangular cleavage tip that has partially been flattened by polishing and machining. Apparently, the defects of a yet unknown origin heavily disturb the machining process and prevented a controlled removal of (111) layers. The observation of nanometre-sized cracks in the same region points to the build-up of a huge stress field due to the interaction of the machining tool with the defective region. These cracks appear as branched channels having directions that are not obviously related to any other surface feature. Similar defects are the reason for a high roughness shown on sample f. Here we again find a large cleavage step and adjacent defects of some ten nanometres in diameter. In this case, however, defects appear as pits, and in the upper part of the image, the defect structure

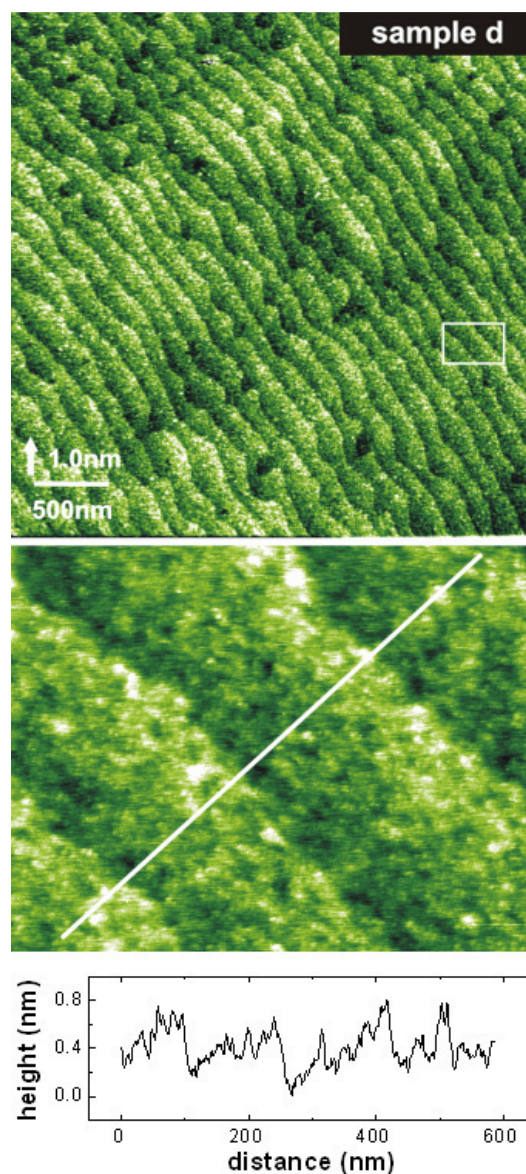


Figure 4. Misalignment of the machining plane and the surface of sample d results in the creation of a vicinal surface composed of a large number of aligned, triple-layer height steps. In this example, the surface inclination is about 5° . A cross-section was taken in a magnified area enclosed by the white rectangle.

heavily disturbed the imaging process so that the topography could not be revealed properly. For a more detailed inspection of such defects, contact mode force microscopy would be more appropriate than the highly sensitive non-contact method used in the present study.

The ultimate goal of precision machining is to create fluorite surfaces with atomic flatness over very large areas and, hence, we explored to what extent machining-related surface structures can be imaged with atomic precision. There is a general difficulty in imaging polished and machined surfaces as they are very rough at a small scale compared to clean *in situ* cleaved samples where atomic resolution imaging in great detail is readily available [8]. For the topographic features being comparable in size with the dimensions of the tip, convolution effects play a major role in NC-SFM imaging of

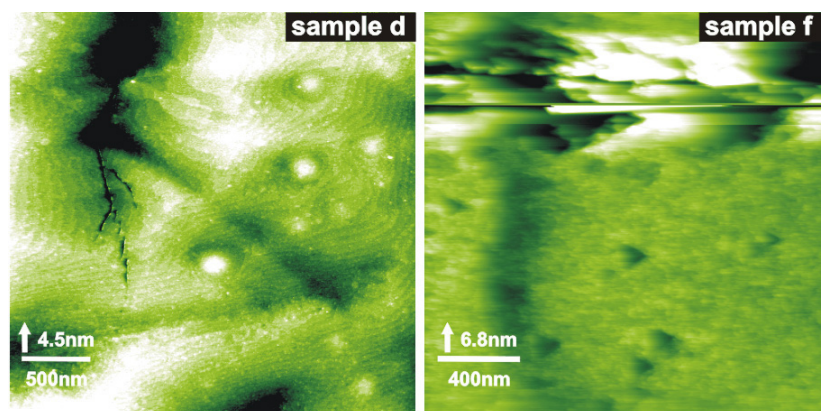


Figure 5. Areas of enhanced roughness as observed in bad areas of samples d and f. On sample d, machining is apparently hampered by large (some nanometres) protruding defects inhibiting controlled material removal in their vicinity. Stress induced by the enhanced interaction of the machining tool with the surface yields micro-cracks. On sample f, pit defects with a depth of some nanometres may also lead to uncontrolled SFM imaging results. The highly sensitive NC-SFM fails to examine a surface area of very high roughness like the one in the upper part of this frame.

polished surfaces. As sketched in figure 6, one cannot assume that only the foremost nanotip contributes to the image contrast but other parts of the tip apex are interacting with the surface. Standard NC-SFM tips with tip radii of ten or more nanometres and with cone angles of 20° may be too coarse in this context. Super-sharp tips as have been introduced recently by different vendors could help to overcome this imaging problem in future studies; however, so far they could not prove their superiority in our experimental setup.

4. Conclusions

We demonstrate that $\text{CaF}_2(111)$ surfaces can successfully be processed to close to atomic flatness over very large areas. The resulting RMS roughness is typically 0.3 nm. While conventional large area surface analysis tools can only give very general information on surface quality, dynamic scanning force microscopy allows a detailed investigation of surface topography on the nanometre and sub-nanometre scales. The high resolution obtained with the NC-SFM allows a clear identification of the origin of the residual surface roughness as being due to jumps of ± 1 triple-layer of the $\text{CaF}_2(111)$ surface.

Furthermore, our results allow a clear distinction between material defects and machining faults. Material defects may, however, prevent proper cleavage of the $\text{CaF}_2(111)$ surface and may influence subsequent machining steps. On the other hand, machining faults like a small inclination between the surface and machining plane may result in terraced structures or contamination of the surface. It is still unclear how and why the observed ridges are formed during the machining process. In further studies we aim for an increase in resolution to eventually be capable of imaging the topography and chemical properties of technical fluorite surfaces with atomic precision.

Acknowledgments

Support from the Deutsche Forschungsgemeinschaft and the Japan Society for the Promotion of Sciences is gratefully acknowledged.

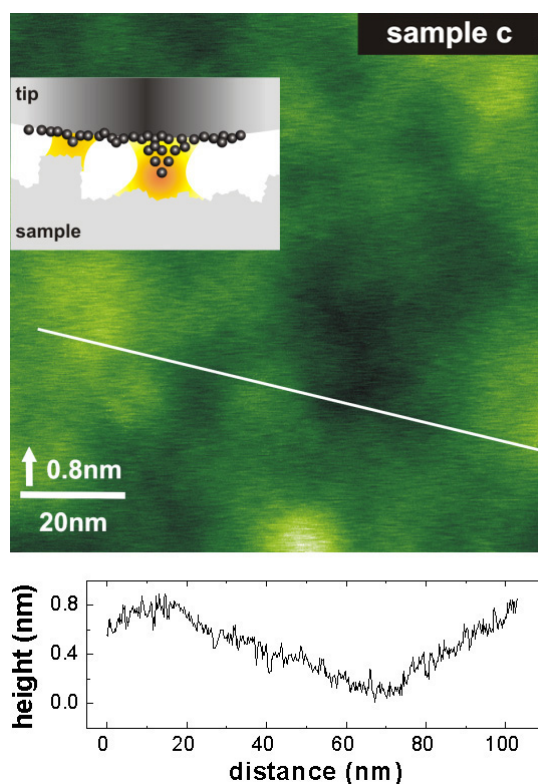


Figure 6. Highest resolution image taken in a very flat region of sample c. The size of the apparent surface features is determined by smearing effects due to the finite radius of the tip apex, as schematically illustrated by the inset. An interaction with more than one cluster may contribute to the total tip-sample interaction.

References

- [1] Bloomstein T M, Liberman V, Rothschild M, Hardy D E and Goodman R B 1999 *Proc. SPIE—Int. Soc. Opt. Eng.* **3676** 342
- [2] Lerner E J 1999 *Ind. Phys.* **5** 18
- [3] Rothschild M *et al* 1999 *J. Vac. Sci. Technol. B* **17** 3262
- [4] Burnett J H, Levine Z H and Shirley E L 2001 *Phys. Rev. B* **64** 241102

-
- [5] Liberman V, Bloomstein T M, Rothschild M, Sedlacek J H C, Uttaro R S, Bates A K, Van Peski C and Orvek K 1999 *J. Vac. Sci. Technol. B* **17** 3273
- [6] Letz M 2004 *Phys. J.* **3** 43
- [7] Namba Y, Ohnishi N, Yoshida S, Harada K and Yoshida K 2004 *CIRP Ann.* **53** 459
- [8] Barth C, Foster A S, Reichling M and Shluger A L 2001 *J. Phys.: Condens. Matter* **13** 2061
- [9] Namba Y, Wada R, Unno K and Tsuboi A 1989 *CIRP Ann.* **38** 331
- [10] Namba Y, Tsuwa H and Wada R 1987 *CIRP Ann.* **36** 211
- [11] Barth C and Reichling M 2000 *Surf. Sci.* **470** L99